Analytical Biochemistry 658 (2022) 114927

Contents lists available at ScienceDirect

Analytical Biochemistry

journal homepage: www.elsevier.com/locate/yabio

High throughput analysis of vacuolar acidification

Chi Zhang [a], Adam Balutowski [a,1], Yilin Feng [a], Jorge D. Calderin [a], Rutilio A. Fratti [a,b,*]

[a] Department of Biochemistry, University of Illinois Urbana-Champaign, Urbana, IL, 61801, USA
[b] Center for Biophysics and Quantitative Biology, University of Illinois Urbana-Champaign, Urbana, IL, 61801, USA

ARTICLE INFO

Keywords:
V-ATPase
Vph1
Lysosome
Acridine orange
Lanthanum
Gadolinium
Nickel

ABSTRACT

Eukaryotic cells are compartmentalized into membrane-bound organelles, allowing each organelle to maintain the specialized conditions needed for their specific functions. One of the features that change between organelles is lumenal pH. In the endocytic and secretory pathways, lumenal pH is controlled by isoforms and concentration of the vacuolar-type H^+-ATPase (V-ATPase). In the endolysosomal pathway, copies of complete V-ATPase complexes accumulate as membranes mature from early endosomes to late endosomes and lysosomes. Thus, each compartment becomes more acidic as maturation proceeds. Lysosome acidification is essential for the breakdown of macromolecules delivered from endosomes as well as cargo from different autophagic pathways, and dysregulation of this process is linked to various diseases. Thus, it is important to understand the regulation of the V-ATPase. Here we describe a high-throughput method for screening inhibitors/activators of V-ATPase activity using Acridine Orange (AO) as a fluorescent reporter for acidified yeast vacuolar lysosomes. Through this method, the acidification of purified vacuoles can be measured in real-time in half-volume 96-well plates or a larger 384-well format. This not only reduces the cost of expensive low abundance reagents, but it drastically reduces the time needed to measure individual conditions in large volume cuvettes.

1. Introduction

Eukaryotic cells are subdivided and organized into membrane-bound organelles that have distinct sets of enzymes and molecules to serve in organelle-specific roles [1,2]. Organelles communicate through the budding, trafficking, and fusion of transport vesicles containing lumenal or membrane integrated cargo. In the endolysosomal pathway, cargo is transferred from early endosomes to late endosomes and ultimately lysosomes. Upon delivery to lysosomes macromolecular cargo is broken down into building blocks by various digestive enzymes, which are activated by the acidification of the lysosomal lumen [2–6].

One of the major characteristics that distinguishes early endosomes from late endosomes and lysosomes is the gradual decrease of pH. As endosomes mature, the lumenal pH drops from 6.5 in early endosomes to 5.5 in late endosomes, while lysosomal compartments acidify to a range between 4 and 5, depending on the organism [2,6–8]. Lumenal acidification is required in the activation of and function of lysosomal digestive enzymes to breakdown proteins, lipids, toxins as endosomal cargo, and entire organelles delivered to lysosomes through autophagy [2,6–9]. The principal source of vesicle acidification is vacuolar-type H^+-ATPase (V-ATPase) that is composed of two protein sub-complexes. The V_O sub-complex is imbedded in the membrane and contains the c-ring that binds and releases H^+. As it rotates the c-ring encounters the two hemi-channels of the a-subunit that face the cytosol and vesicle lumen. The cytosolic hemi-channel loads the H^+ on to the c-ring and the lumenal hemi-channel releases the H^+ into the vesicle lumen. The energy used to transfer H^+ through the V_O against a concentration gradient comes from the cytoplasmic V_1 complex containing the ATPase activity of the enzyme. When assembled, the V_1-V_O holocomplex uses ATP hydrolysis to turn the c-ring and pump H^+ into the lysosomal lumen [2,10,11]. The importance of lysosomal acidification is broad. Not only can defective acidification lead to the accumulation of immature hydrolytic enzymes, but deficient V-ATPase activity has been linked to reduced autophagy, lysosomal storage disorders, Alzheimer's Disease, Parkinson's Disease, and more [8,10,12,13].

Since the process of endosome maturation and endocytosis is evolutionarily conserved in eukaryotic cells, it is advantageous to study the lysosomal fusion pathway and V-ATPase function in the budding

Abbreviations: AO, acridine orange; FCCP, Carbonyl cyanide-4-(trifluoromethoxy) phenylhydrazone; TRP, Transient Receptor Potential.

* Corresponding author. University of Illinois at Urbana-Champaign, 430 Roger Adams Laboratory 600 S, Mathews Ave. Box B4, MC712, Urbana, IL, 61801, USA.
E-mail address: rfratti@illinois.edu (R.A. Fratti).
[1] Current address: Biochemistry, Biophysics, and Structural Biology program, Washington University, St. Louis, MO.

https://doi.org/10.1016/j.ab.2022.114927
Received 13 August 2022; Received in revised form 9 September 2022; Accepted 20 September 2022
Available online 24 September 2022
0003-2697/

yeast *Saccharomyces cerevisiae*. One of the advantages of using *S. cerevisiae* vacuolar lysosomes is the ease of their isolation at high concentrations. Vacuoles isolated from 1 L of medium can yield upwards of 1 mg of vacuoles by protein. Importantly, these organelles contain all the essential proteins and lipids for *in vitro* analysis of fusion, fission, Ca^{2+} transport, actin polymerization and V-ATPase activity [11,14–18]. Furthermore, the relative ease and low cost of yeast genetics makes it easy to introduce gene deletions, mutations, truncations, and chimeras to further probe cellular functions including vacuole acidification [19,20]. A common method to quantify yeast vacuole acidification uses the fluorescein derivative BCECF-AM (2′,7′ –bis-(Carboxyeth yl)-5-(and-6)-carboxyfluorescein-acetoxymethyl ester), a pH-sensitive fluorescent probe that labels mammalian cytosol and accumulates in yeast vacuoles. BCECF fluoresces at two excitation wavelengths. While excitation at 440 nm is not affected by pH, it does affect excitation at 490 nm. Ratios of emission at 535 nm are taken with each excitation point to calculate the pH of vacuole lumen [21–24]. Other dyes, including Oregon Green, fluorescein derivatives, and HPTS (8-hydroxypyrene-1,2,3-trisulfonic acid), pHrodo, as well as the pH sensitive GFP derivative pHlourin have been used in fluorescently labeling lysosomes of mammalian cells [25–33]. These assays, however, measures the lysosome pH *in vivo*, which is not ideal for high-throughput studies of V-ATPase function. This is due to the need to feed cells dextran conjugates of pH sensitive dyes or genetic expression of pHlouorin. For our high-throughput *in vitro* assay we used the fluorescent dye Acridine Orange (AO) which readily accumulates in acidified isolated vacuoles *in vitro* [34–36].

AO has two dominant absorption peaks at 460 nm and 540 nm and the difference in absorbance has been used as a measure of vacuole acidification [34,37]. Using this difference in absorbance, others have used AO to measure *in vitro* yeast vacuole acidification in single read reactions using large volume cuvettes, which can be laborious and can limit the number of variables tested per vacuole preparation. Instead of relying on a difference in absorbance, we take advantage of changes in fluorescence intensity in a microtiter plate format.

AO fluoresces with a peak emission at 520 nm when excited at 488 nm [38,39] and stains double-stranded DNA with the expected green color, but stains single-stranded DNA and RNA with red color [40–43]. The reason for the two AO emission wavelengths is because of its metachromatic shift. When AO is accumulated, the increase of local concentration of AO pushes monomers to dimerize through base stacking, and the dimerization leads to a shift in dominant emission peak from 520 nm to 680 nm [39,40,44,45]. When AO is used to stain acidic compartments *in vivo*, AO monomers pass through membranes and become trapped in acidic compartments upon protonation to fluorescently label them [43,44].

Here we present a high-throughput *in vitro* assay using AO fluorescence and half-volume 96 well plates (i.e., 192 well plate equivalent) that can be scaled to a 384-well format. Upon the addition of ATP, the V-ATPase transports H^+ from the reaction buffer system to the vacuole lumen and changes in fluorescence are measured with an excitation of 485 nm and emission at 520 nm. As V-ATPase complexes hydrolyze ATP to pump H^+ into the vacuole lumen, AO accumulates in the acidic vacuoles, which causes to a shift in emission wavelength from 520 nm to 680 nm due to AO dimerization [38,39,44], therefore a gradual decrease of fluorescence signals at emission wavelength of 520 nm is observed. Thus, a larger decrease of AO fluorescence indicates greater vacuolar acidification.

2. Experimental

2.1. Chemicals/reagents

Soluble reagents were dissolved in PIPES-Sorbitol (PS) buffer (20 mM PIPES-KOH, pH 6.8, 200 mM sorbitol) with 125 mM KCl unless indicated otherwise. ATP was purchased from RPI (Mount Prospect, IL). Bafilomycin A1 and Concanamycin A were from Cayman Chemical (Ann Arbor, MI) and dissolved in DMSO. Acridine orange, Coenzyme A (CoA), Creatine kinase, and FCCP (Carbonyl cyanide-4-(trifluoromethoxy) phenylhydrazone) were purchased from Sigma (St. Louis, MO). Creatine phosphate was from Abcam (Waltham, MA). Pbi2 (Proteinase B inhibitor 2) was prepared as described and dialyzed against PS buffer with 125 mM KCl [46]. IgG preparations of anti-Sec17 were made as described and dialyzed against PS buffer with 125 mM KCl [47]. The PH domain of FAPP1 was expressed as an MBP fusion and dialyzed against PS buffer with 125 mM KCl as described [48].

2.2. Yeast strains

Vacuoles from BJ3505 genetic backgrounds were used for H^+ transport assays. *VPH1* was deleted by homologous recombination using PCR products amplified from the pAG32 plasmid with primers 5′-VPH1-KO (5’ – GCTTAGAGGGCTACCTGTGTGTATTTGCA TGGGTAAAAAGCCTGAACTCACC – 3′) and 3′-VPH1-KO (5’ – AGTCCT-CAAAATTTAGCTTGAAGCGGTTATT CCTTTGCCCTCGGACGAGTG – 3) with homology flanking the *VPH1* coding sequence. The PCR product was transformed into chemically competent yeast by standard lithium acetate methods and plated on YPD containing Hygromycin (200 μg/ml) to generate BJ3505 *vph1::hphMX4*.

2.3. Vacuole isolation and vacuole acidification

Vacuoles were isolated as described [49]. The proton pumping activity of isolated vacuoles was performed as described by others with modifications [50,51]. *In vitro* H^+ transport reactions (60 μl) contained 20 μg vacuoles from BJ3505 backgrounds, reaction buffer (20 mM PIPES-KOH pH 6.8, 200 mM sorbitol, 125 mM KCl, 5 mM $MgCl_2$), ATP regenerating system (1 mM ATP, 0.1 mg/ml creatine kinase, 29 mM creatine phosphate), 10 μM CoA, 283 nM Pbi2, and 15 μM of the fluorescent dye AO. Reaction mixtures were loaded into a black, half-volume 96-well flat-bottom plate with nonbinding surface (Corning). ATP regenerating system or buffer was added, and reactions were incubated at 27 °C while AO fluorescence was monitored. Samples were analyzed in a fluorescence plate reader (POLARstar Omega, BMG Labtech) with the excitation filter at 485 nm and emission filter at 520 nm. Reactions were initiated with the addition of ATP regenerating system 20 s after the initial measurement. After the fluorescence drop plateaus were reached, we added 30 μM FCCP to collapse the proton gradient and restore acridine orange fluorescence.

2.4. Statistical analysis

Results are expressed as the mean ± S.E.M. Experimental replicates (n) is defined as the number of separate experiments. Significant differences were calculated using One-Way ANOVA for multiple comparisons using Prism 9 (GraphPad, San Diego, CA). P values ≤ 0.05 were considered significant.

3. Results and discussion

To develop a high-throughput assay for V-ATPase function we first set parameters to detect vacuole acidification in an ATP-dependent manner in the absence of cytosol. For this we isolated vacuoles from exponentially growing yeast and used conditions that favor vacuole fusion [34,51]. Upon addition of ATP regenerating system, a rapid drop in AO fluorescence was measured that plateaued after 600 s (Fig. 1A). In contrast, the reaction lacking ATP did not change in fluorescence intensity, indicating that the observed signal was ATP-dependent. After 600 s had elapsed, 30 μM FCCP was added to each reaction to equilibrate H^+ levels across the vacuole membrane and restore starting fluorescence at 520 nm [52]. This shows that the fluorescence decrease at the beginning of the assay is due to accumulation of AO into lysosomes

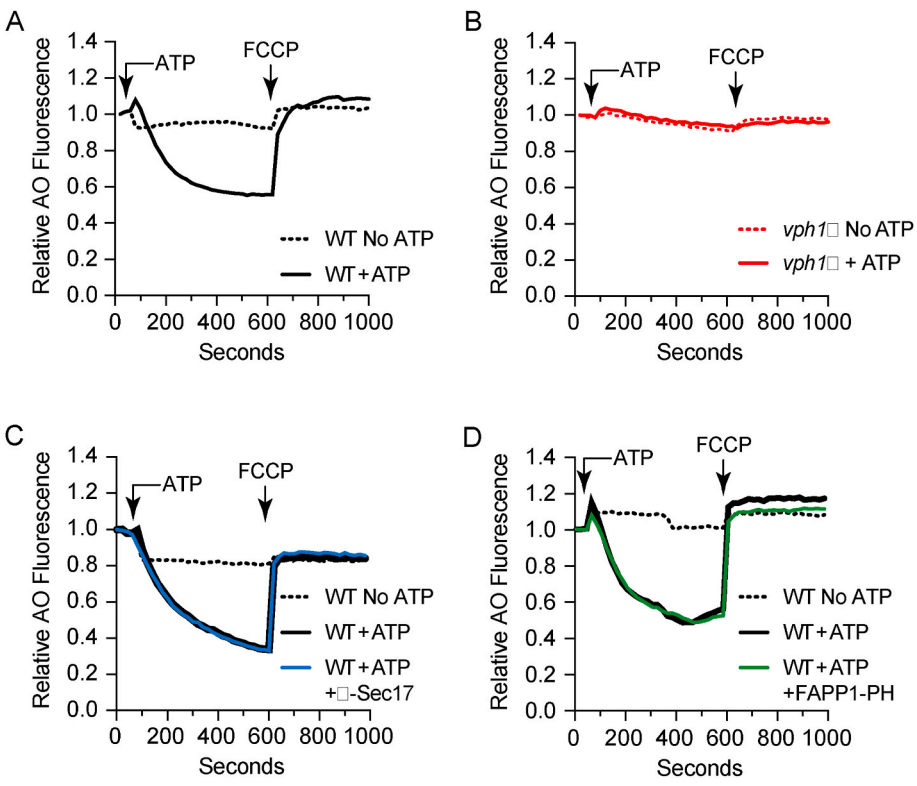

Fig. 1. ATP dependent *in vitro* vacuole acidification. Vacuoles were isolated from wild type **(A, C, D)** and *vph1*Δ **(B)** yeast and used for proton pumping activity measured by the loss of AO fluorescence at 520 nm. **(C)** Wild type vacuoles were incubated with or without 20 μg/ml anti-Sec17 IgG to block SNARE activation. **(D)** Wild type vacuoles were incubated with 1 μM FAPP1-PH to block PI4P and vacuole fusion. Reactions were incubated with or without ATP regenerating system added at 30 s and the reactions were incubated for 600 s. After ~600 s reactions were supplemented with 30 μM FCCP was added to collapse the proton gradient and restore AO fluorescence.

followed by its dimerization.

Next, we verified whether the decrease in AO fluorescence was dependent on V-ATPase function. To determine this, we used vacuoles isolated from yeast where the V_O subunit *VPH1* had been deleted. Others have shown that the Vph1 isoform Stv1 (from the secretory path V-ATPase) can replace Vph1 in the endolysosomal population of the V-ATPase. However, Stv1 does not support vacuolar acidification unless it is overexpressed [53]. This is likely due to the differential regulation of Stv1 and Vph1 by the lipids phosphatidylinositol 4-phosphate (PI4P) and PI(3,5)P_2, respectively [54,55]. Here we see that *vph1*Δ vacuoles were unable to acidify in the presence or absence of ATP, indicating that the drop in AO fluorescence was due to V-ATPase function (Fig. 1B).

The conditions used here are favorable for vacuole homotypic fusion, meaning that there is an abundance of ATP through the use of an ATP regenerating system and physiological K^+ levels. Cytosol is not required and Pbi2 is used as a protease inhibitor. Thus, vacuoles in Fig. 1A are undergoing the early stages of fusion, whereas *vph1*Δ vacuoles are fusion incompetent [34]. To show that the change in AO fluorescence is not due to blocked fusion, we used antibody against the SNARE co-chaperone Sec17 (mammalian α/β/γ-SNAP) [56]. The AAA + Sec18 (mammalian NSF) hydrolyses ATP to disassemble inactive SNARE bundles using Sec17 as a molecular crowbar [57–59]. Blocking Sec17 stops SNARE activation to stop vacuole fusion [60–63]. Here we show that adding anti-Sec17 IgG to AO fluorescence assays had no effect on vacuole acidification (Fig. 1C). This indicates that the loss of fluorescence was not due to vacuole fusion.

To further show that fusion is not the cause of changes in AO fluorescence we used the plekstrin homology (PH) lipid binding domain from FAPP1 [64]. The FAPP1-PH binds to PI4P to block HOPS function and vacuole fusion [48,65,66]. Importantly, PI4P is required for Golgi localized V-ATPase where Stv1 takes the place of Vph1. Stv1 binds PI4P whereas Vph1 binds PI(3,5)P_2 [54,55]. Here we used MBP-FAPP1-PH at levels that block vacuole fusion, yet we observed no change in AO fluorescence (Fig. 1D). This indicated that vacuole was acidified while fusion was inhibited.

While the deletion of *VPH1* does inhibit V-ATPase activity, it is also possible that there are secondary effects that could indirectly affect vacuole acidification. To show that V-ATPase function was directly responsible for the ATP-dependent drop in AO signal, we used two well-characterized inhibitors of the holocomplex. Using wild type vacuoles we tested the effects of Bafilomycin A1 and Concanamycin A that block H^+ translocation by binding to the c-ring of the V_O complex [67,68]. Because both inhibitors are dissolved in DMSO we also tested the solvent to see if any observed effects were due to DMSO and not the solutes. In Fig. 2 we show that both Bafilomycin A1 and Concanamycin A fully blocked the drop in AO fluorescence, while DMSO had no effect. These results, along with the data from the *vph1*Δ vacuoles show that the V-ATPase was indeed the reason for the drop in AO fluorescence due to vacuole acidification.

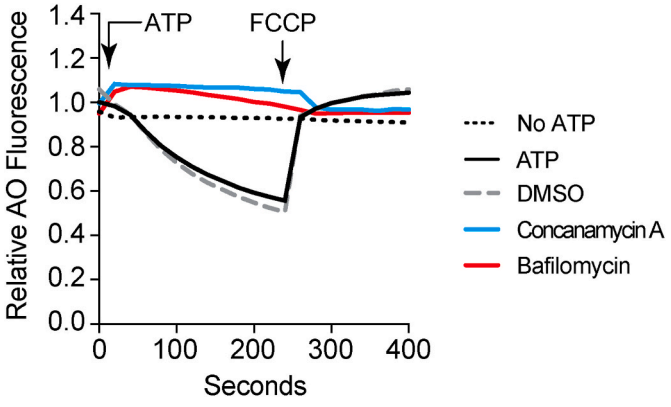

Fig. 2. Bafilomycin A1 and Concanamycin prevent vacuole acidification, Vacuoles were isolated from wild type yeast and used for proton pumping activity measured by the loss of AO as described in Fig. 1. Reactions were incubated with or without ATP. Reactions containing ATP were treated with PS buffer, 100 nM Bafilomycin, 100 nM Concanamycin or an equivalent of solvent (DMSO). Reactions were incubated for 250 s before adding FCCP. Readings continued for 400 s.

Next, we tested if lowering the pH of the vacuole lumen, in the presence of a functioning V-ATPase, would block AO from shifting in fluorescence. To do this we used the weak base chloroquine, which accumulates in acidic compartments as it is protonated [69,70]. As a result, the lumenal pH increases, which would result in a decrease in AO protonation and trapping in the lysosome. This would in turn fail to raise the local concentration of AO in the lysosomes to promote its dimerization and subsequent emission shift. Here we show that AO fluorescence increased as chloroquine concentrations were raised (Fig. 3). This also shows that AO fluorescence can gradually decrease in a dose dependent manner.

Finally, we used the high-throughput AO assay to screen for novel inhibitors of V-ATPase function. Previously we found that 100 μM Cu^{2+} potently inhibited vacuole acidification, whereas other divalent cations tested had no effect [51]. Here we tested various metals simultaneously to show how the assay can accommodate numerous conditions in a single reading. We tested the lanthanide cations La^{3+} and Gd^{3+} as well as the divalent cation Ni^{2+}. When we added $LaCl_3$ and $GdCl_3$ to the acidification assay there was a pronounced increase in AO fluorescence in a dose-dependent manner. This was not due to vacuole lysis as fluorescence was restored to baseline when H^+ was equilibrated across the vacuole membrane with the protonophore FCCP (Fig. 4A–D). In contrast to the lanthanides, divalent Ni^{2+} inhibited vacuole acidification in a manner similar to what was seen with Cu^{2+} (Fig. 4E and F). This was also consistent with a study showing that Ni^{2+} reduced proton pumping by isolated rat liver lysosomes containing endocytosed fluorescein dextran [71].

The increase in AO fluorescence due to La^{3+} and Gd^{3+} was unexpected. A block in acidification typically manifests in a lack in AO fluorescence decrease at 520 nm as we saw with Ni^{2+} treated reactions. What would cause AO to increase in fluorescence? We hypothesize that this could be linked to the effects of lanthanides on Ca^{2+}-ATPases and Ca^{2+} channels. Yeast vacuoles take in Ca^{2+} using the Ca-ATPase Pmc1 and the Ca^{2+}/H^+ antiporter [72,73]. Ca^{2+} is released from vacuoles through the TRP (Transient Receptor Potential) homolog Ca^{2+} channel Yvc1 [74]. Yvc1 releases Ca^{2+} from the vacuole lumen during osmotic shock, when surface exposed Cys are modified with glutathione by Gtt1, which is likely to disrupt Yvc1 dimers and promote Ca^{2+} release [15,74–76]. Therefore, Yvc1 is unlikely involved here because it is not active under the isotonic conditions of the assay. Another unidentified Ca^{2+} release mechanism has been detected that operates under isotonic conditions in a SNARE dependent manner and in the absence of Yvc1 [15,61].

Lanthanides can have effects on surface charge, dipole potential, and

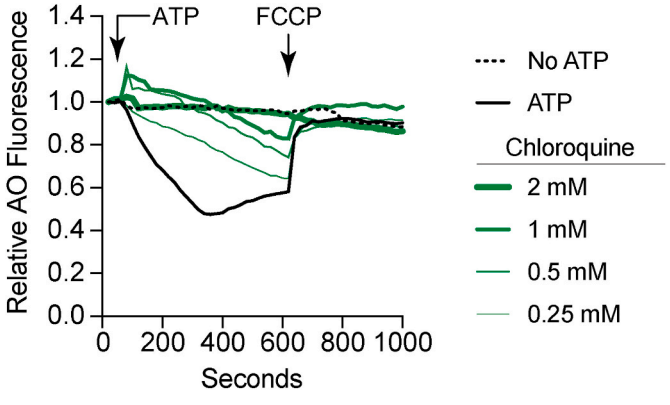

Fig. 3. Chloroquine prevents the loss of AO fluorescence. Vacuoles were isolated from wild type yeast and used for proton pumping activity measured by the loss of AO as described in Fig. 1. Reactions were incubated with or without ATP. Reactions containing ATP were treated with PS buffer or chloroquine at the indicated concentrations. Reactions were incubated for 600 s before adding FCCP. Readings continued for 1000 s.

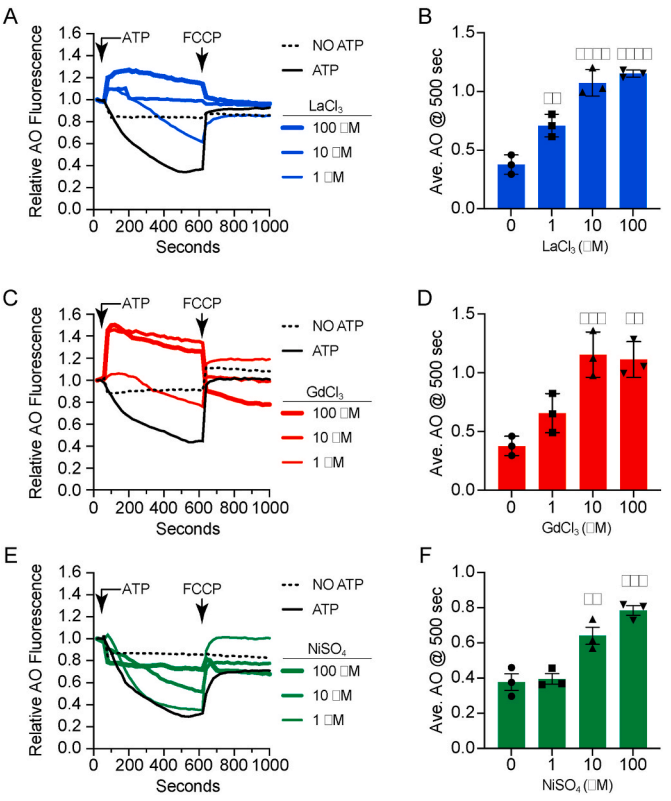

Fig. 4. Effect of metals on AO fluorescence. Vacuoles were isolated from wild type yeast and used for proton pumping activity measured by the loss of AO as described in Fig. 1. Reactions were incubated with or without ATP. Reactions containing ATP were treated with PS buffer or $LaCl_3$ **(A–B)**, $GdCl_3$ **(C–D)** or $NiSO_4$ **(E–F)** at the indicated concentrations. Reactions were incubated for 600 s before adding FCCP. Readings continued for 1000 s. All conditions **(A, C, E)** were run in the same plate each of the three repeats and shared the same 0 μM control. Error bars are S.E.M. (n = 3). $^{**}p < 0.01$, $^{***}p < 0.001$, $^{****}p < 0.0001$ (One way ANOVA for multiple comparisons).

transmembrane potential that can affect different types of Ca^{2+} transporters [77]. For instance, Gd^{3+} has been shown to interact with phosphatidylserine and augment dipole potential resulting in increased membrane tension due to enhanced packing of lipids. This can subsequently inhibit the function of mechanosensitive channels including the mucolipin Ca^{2+} channel TRPML [78]. In addition, La^{3+} and Gd^{3+} can activate or potentiate the function of other TRP family members including TRPV1 [79]. Importantly, plasma membrane Ca-ATPase (PMC) family members as well as some TRP families can be inhibited by lanthanides [79–81]. The effects of La^{3+} and Gd^{3+} seen here are unlikely to be dependent on the release of Ca^{2+} by Yvc1 for the reasons listed above.

Regarding the connection between Ca^{2+} transport and vesicle acidification, we and others have shown that a Ca^{2+} gradient is needed for vacuole/lysosome acidification to occur normally [82,83]. Based on the need for a Ca^{2+} gradient for vacuole acidification to occur, any effects of La^{3+} and Gd^{3+} on acidification through Ca^{2+} would have to target uptake mechanisms [83]. Notably, in addition to channels, lanthanides can also block Ca^{2+}-ATPase pumps [80,84]. In this scenario a block in acidification would depend on the build-up of Ca^{2+} outside of the vacuole lumen. Importantly, adding exogenous excess Ca^{2+} does block vacuole acidification [82].

As mentioned, lanthanides can affect Ca-ATPase pumps at the plasma membrane as well as the endoplasmic reticulum. Both Gd^{3+} and La^{3+} induce conformational changes in SERCA to block Ca^{2+} transport [85]. Thus, it is likely that Pmc1 function is altered by lanthanides in a similar manner. If La^{3+} and Gd^{3+} inhibited Pmc1, the extralumenal Ca^{2+} would

enter through the low affinity Ca^{2+}/H^{+} antiporter Vcx1 [73]. Uptake through Vcx1 would result in the release of H^{+} from the vacuole lumen. Alternatively, La^{3+} and Gd^{3+} could block both Pmc1 and Vcx1 leading to the lack of Ca^{2+} gradient that could in turn inhibit V-ATPase function. In either case, H^{+} would not accumulate in the vacuole lumen. The ionic strength of La^{3+} and Gd^{3+} could keep AO from entering the vacuole, which could lead to AO protonation (AOH) while outside the vacuole. Protonation of AO would prevent its entry into the vacuole lumen where it would normally dimerize ($[AOH]_2$) and fluoresce at 680 nm. Instead, the increased extralumenal AOH would shift to the monomeric form leading to the observed increased fluorescence at 530 nm. Clearly, these results are only the beginning of a new set of experiments that are beyond the scope of a methods paper. Thus, the hypothesis is only a discussion point at this time.

4. Conclusion

Here we show the adaptation of a large volume single sample assay of vacuole acidification to a high-throughput microtiter plate format. Classically, acidification was show by shifts in absorbance of AO or fluorescence quenching of ACMA (9-amino-6-chloro-2-methoxyacridine) in cuvettes holding as much as 3 ml per reaction [34,52,86–88]. Cuvette based assays limit the amounts of conditions that can be tested with a single organelle preparation. For example, if each reaction were run for 10 min, the researcher would be limited to six reactions in an hour. Meanwhile, we routinely run 30–40 reactions at the same time. Not only does this save time but reading reactions in parallel also ensures that you are comparing apples to apples. Purified organelles have a limited lifetime and can only be used for 1–2 h before they stop functioning well. Even comparing vacuoles an hour apart can change the kinetics in a functional assay. Taking this into consideration, the investigator using back-to-back cuvette readings will be looking at different vacuoles between the first reaction and the sixth. Using this limitation as an impetus, we scaled this assay down to 30 or 60 μl to fit in 384-well or 96 half-volume microtiter plates, respectively. This format allows for the screening of numerous reagents and conditions in a single round, which is of particular importance if testing low abundance and expensive reagents such antibodies. This also allows for the side-by-side comparison of genetic mutations and their wild-type parent.

Like most assays, there are limitations to what can be tested with this format. For instance, there is a maximum amount of DMSO and other organic solvents that can be used without damaging the vacuoles. As such, we have been unable to test specific small molecule inhibitors due to solvent effects. Other limitations can come from interfering with the reporter itself. Some small molecule inhibitors quench AO fluorescence in the absence of vacuoles. Thus, it is important to make sure that the reagents being tested do not indirectly interfere with membrane integrity or the reporter system. Finally, there is the matter of quantitation. AO fluorescence is not a specific measure of pH in each organelle. This is meant a qualitative measure of acidification. More specific readings of pH would require fluorophores that can be calibrated with a pH curve including FITC and pHluorin. Naturally, this has its limitations as well, as it cannot be easily converted to a rapid high throughput format.

Can this AO assay be used using whole cells? The short answer is yes, but there will be a need for additional controls and considerations. With yeast, the dye would have to travel through the cell wall and plasma membrane before gaining access to the vacuole. This would add time to when fluorescence changes are expected. As for controls, we must remember that AO also binds DNA and RNA with different emissions. This signal would have to be subtracted from signal originating from acidified compartments. One way to do this is to run a control sample that uses Bafilomycin or some other compound to prevent lysosome/vacuole acidification. AO would still be able to label DNA and RNA to give a subtractable signal. This being said, we have not adapted the assay to use whole cells and doing so would require a new methods study.

Finally, it is important to consider anion flux when examining V-ATPase mediated acidification. Producing a pH gradient by V-ATPase creates an electrical current that requires a counterion. In the endolysosomal pathway, Cl^{-} ions are transported into vesicles through the CLC family some of which act as channels while other function as antiporters that exchange $1H^{+}$ for $2Cl^{-}$ [89]. Vesicle pH can also be affected by other antiporters from the $Na^{+}(K^{+})/H^{+}$ exchangers family including NHE6 in mammalian cells and Nhx1 in yeast [23,90,91]. Thus, when screening for regulators of V-ATPase function, it is important to consider other proteins that could be the true target of a discovered molecule. Lastly, one must be aware of the effects of different anions on maintaining a H^{+} gradient. For instance, H^{+} gradients can be altered by some anions without affecting V-ATPase activity. At physiological concentrations of K^{+} (150 mM), the counterion Cl^{-} can lead to a faster loss of a H^{+} gradient compared to the effects of $SO4^{-}$ [92].

Author contribution

C.Z., A.B., R.A.F. conceptualization, C.Z., A.B. Y.F. J.D.C. data curation; C.Z., A.B., R.A.F. formal analysis; C.Z., R.A.F. writing original draft; C.Z., R.A.F. writing rereview and editing; R.A.F. funding acquisition; R.A.F. supervision; R.A.F. project administration; R.A.F. resources.

Declaration of competing interests

The authors declare that they do not have conflicts of interest with the contents of this article.

Data availability

Data will be made available on request.

Acknowledgments

This research was supported by grants from the National Science Foundation (MCB 1818310, MCB 2216742) to RAF. J.D.C. was partially supported by an NIGMS-NIH Chemistry-Biology Interface Training Grant (5T32-GM070421).

References

[1] C.P. Satori, M.M. Henderson, E.A. Krautkramer, V. Kostal, M.D. Distefano, M. M. Distefano, E.A. Arriaga, Bioanalysis of eukaryotic organelles, Chem Rev 113 (2013) 2733–2811, https://doi.org/10.1021/cr300354g.
[2] M. Thattai, Organelle acidification: an ancient cellular leak detector, BMC Biol. 15 (2017) 51, https://doi.org/10.1186/s12915-017-0395-1.
[3] Y.-B. Hu, E.B. Dammer, R.-J. Ren, G. Wang, The endosomal-lysosomal system: from acidification and cargo sorting to neurodegeneration, Transl. Neurodegener. 4 (2015) 18, https://doi.org/10.1186/s40035-015-0041-1.
[4] R.M. Steinman, I.S. Mellman, W.A. Muller, Z.A. Cohn, Endocytosis and the recycling of plasma membrane, J. Cell Biol. 96 (1983) 1–27, https://doi.org/10.1083/jcb.96.1.1.
[5] J.M. Besterman, R.B. Low, Endocytosis: a review of mechanisms and plasma membrane dynamics, Biochem. J. 210 (1983) 1–13, https://doi.org/10.1042/bj2100001.
[6] J. Huotari, A. Helenius, Endosome maturation, EMBO J. 30 (2011) 3481–3500, https://doi.org/10.1038/emboj.2011.286.
[7] F.R. Maxfield, T.E. McGraw, Endocytic recycling, Nat. Rev. Mol. Cell Biol. 5 (2004) 121–132, https://doi.org/10.1038/nrm1315.
[8] Y.-B. Hu, E.B. Dammer, R.-J. Ren, G. Wang, The endosomal-lysosomal system: from acidification and cargo sorting to neurodegeneration, Transl. Neurodegener. 4 (2015) 18, https://doi.org/10.1186/s40035-015-0041-1.
[9] C. Wang, T. Zhao, Y. Li, G. Huang, M.A. White, J. Gao, Investigation of endosome and lysosome biology by ultra pH-sensitive nanoprobes, Adv. Drug Deliv. Rev. 113 (2017) 87–96, https://doi.org/10.1016/j.addr.2016.08.014.
[10] L. Stransky, K. Cotter, M. Forgac, The function of V-ATPases in cancer, Physiol. Rev. 96 (2016) 1071–1091, https://doi.org/10.1152/physrev.00035.2015.
[11] T.L. Baars, S. Petri, C. Peters, A. Mayer, Role of the V-ATPase in regulation of the vacuolar fission-fusion equilibrium, Mol. Biol. Cell 18 (2007) 3873–3882, https://doi.org/10.1091/mbc.e07-03-0205.
[12] D.J. Colacurcio, R.A. Nixon, Disorders of lysosomal acidification-The emerging role of v-ATPase in aging and neurodegenerative disease, Ageing Res. Rev. 32 (2016) 75–88, https://doi.org/10.1016/j.arr.2016.05.004.

[13] Q. Song, B. Meng, H. Xu, Z. Mao, The emerging roles of vacuolar-type ATPase-dependent Lysosomal acidification in neurodegenerative diseases, Transl. Neurodegener. 9 (2020) 17, https://doi.org/10.1186/s40035-020-00196-0.

[14] W. Wickner, Membrane fusion: five lipids, four SNAREs, three chaperones, two nucleotides, and a Rab, all dancing in a ring on yeast vacuoles, Annu. Rev. Cell Dev. Biol. 26 (2010) 115–136, https://doi.org/10.1146/annurev-cellbio-100109-104131.

[15] G.E. Miner, K.D. Sullivan, C. Zhang, D. Rivera-Kohr, A. Guo, L.R. Hurst, E.C. Ellis, M.L. Starr, B.C. Jones, R.A. Fratti, Phosphatidylinositol 3,5-bisphosphate regulates Ca2+ transport during yeast vacuolar fusion through the Ca2+ ATPase Pmc1, Traffic 21 (2020) 503–517, https://doi.org/10.1111/tra.12736.

[16] Z.D. Gokbayrak, D. Patel, C.L. Brett, Acetate and hypertonic stress stimulate vacuole membrane fission using distinct mechanisms, PLoS One 17 (2022), e0271199, https://doi.org/10.1371/journal.pone.0271199.

[17] S. Isgandarova, L. Jones, D. Forsberg, A. Loncar, J. Dawson, K. Tedrick, G. Eitzen, Stimulation of actin polymerization by vacuoles via Cdc42p-dependent signaling, J. Biol. Chem. 282 (2007) 30466–30475, https://doi.org/10.1074/jbc.M704117200.

[18] G.-H. Sun-Wada, Y. Wada, Role of vacuolar-type proton ATPase in signal transduction, Biochim. Biophys. Acta 1847 (2015) 1166–1172, https://doi.org/10.1016/j.bbabio.2015.06.010.

[19] N.R. Adames, J.E. Gallegos, J. Peccoud, Yeast genetic interaction screens in the age of CRISPR/Cas, Curr. Genet. 65 (2019) 307–327, https://doi.org/10.1007/s00294-018-0887-8.

[20] R.M. Giersch, G.C. Finnigan, Yeast still a beast: diverse applications of CRISPR/cas editing technology in S. cerevisiae, Yale J. Biol. Med. 90 (2017) 643–651.

[21] P.J. Plant, M.F. Manolson, S. Grinstein, N. Demaurex, Alternative mechanisms of vacuolar acidification in H(+)-ATPase-deficient yeast, J. Biol. Chem. 274 (1999) 37270–37279, https://doi.org/10.1074/jbc.274.52.37270.

[22] R. Ali, C.L. Brett, S. Mukherjee, R. Rao, Inhibition of sodium/proton exchange by a Rab-GTPase-activating protein regulates endosomal traffic in yeast, J. Biol. Chem. 279 (2004) 4498–4506, https://doi.org/10.1074/jbc.M307446200.

[23] C.L. Brett, D.N. Tukaye, S. Mukherjee, R. Rao, The yeast endosomal Na+K+/H+ exchanger Nhx1 regulates cellular pH to control vesicle trafficking, Mol. Biol. Cell 16 (2005) 1396–1405, https://doi.org/10.1091/mbc.e04-11-0999.

[24] T.T. Diakov, M. Tarsio, P.M. Kane, Measurement of vacuolar and cytosolic pH in vivo in yeast cell suspensions, J Vis Exp (2013), https://doi.org/10.3791/50261.

[25] J. Canton, S. Grinstein, Measuring lysosomal pH by fluorescence microscopy, Methods Cell Biol. 126 (2015) 85–99, https://doi.org/10.1016/bs.mcb.2014.10.021.

[26] P.M. Haggie, A.S. Verkman, Unimpaired lysosomal acidification in respiratory epithelial cells in cystic fibrosis, J. Biol. Chem. 284 (2009) 7681–7686, https://doi.org/10.1074/jbc.M809161200.

[27] B.E. Steinberg, K.K. Huynh, A. Brodovitch, S. Jabs, T. Stauber, T.J. Jentsch, S. Grinstein, A cation counterflux supports lysosomal acidification, J. Cell Biol. 189 (2010) 1171–1186, https://doi.org/10.1083/jcb.200911083.

[28] G. Miesenböck, D.A. De Angelis, J.E. Rothman, Visualizing secretion and synaptic transmission with pH-sensitive green fluorescent proteins, Nature 394 (1998) 192–195, https://doi.org/10.1038/28190.

[29] D.C. Prosser, K. Wrasman, T.K. Woodard, A.F. O'Donnell, B. Wendland, Applications of pHluorin for quantitative, kinetic and high-throughput analysis of endocytosis in budding yeast, J Vis Exp (2016), https://doi.org/10.3791/54587.

[30] C.C. Overly, K.D. Lee, E. Berthiaume, P.J. Hollenbeck, Quantitative measurement of intraorganelle pH in the endosomal-lysosomal pathway in neurons by using ratiometric imaging with pyranine, Proc. Natl. Acad. Sci. U. S. A. 92 (1995) 3156–3160, https://doi.org/10.1073/pnas.92.8.3156.

[31] G.L. Busch, H. Wiesinger, E. Gulbins, H.J. Wagner, B. Hamprecht, F. Lang, Effect of astroglial cell swelling on pH of acidic intracellular compartments, Biochim. Biophys. Acta 1285 (1996) 212–218, https://doi.org/10.1016/s0005-2736(96)00163-0.

[32] C.J. Galloway, G.E. Dean, M. Marsh, G. Rudnick, I. Mellman, Acidification of macrophage and fibroblast endocytic vesicles in vitro, Proc. Natl. Acad. Sci. U. S. A. 80 (1983) 3334–3338, https://doi.org/10.1073/pnas.80.11.3334.

[33] M. Miksa, H. Komura, R. Wu, K.G. Shah, P. Wang, A novel method to determine the engulfment of apoptotic cells by macrophages using pHrodo succinimidyl ester, J. Immunol. Methods 342 (2009) 71–77, https://doi.org/10.1016/j.jim.2008.11.019.

[34] M.J. Bayer, C. Reese, S. Buhler, C. Peters, A. Mayer, Vacuole membrane fusion: V0 functions after trans-SNARE pairing and is coupled to the Ca2+-releasing channel, J. Cell Biol. 162 (2003) 211–222, https://doi.org/10.1083/jcb.200212004.

[35] M.P. D'Souza, S.V. Ambudkar, J.T. August, P.C. Maloney, Reconstitution of the lysosomal proton pump, Proc. Natl. Acad. Sci. U. S. A. 84 (1987) 6980–6984, https://doi.org/10.1073/pnas.84.20.6980.

[36] Y. Moriyama, T. Takano, S. Ohkuma, Acridine orange as a fluorescent probe for lysosomal proton pump, J. Biochem. 92 (1982) 1333–1336, https://doi.org/10.1093/oxfordjournals.jbchem.a134053.

[37] S. Gluck, S. Kelly, Q. Al-Awqati, The proton translocating ATPase responsible for urinary acidification, J. Biol. Chem. 257 (1982) 9230–9233.

[38] F. Nadrigny, D. Li, K. Kemnitz, N. Ropert, A. Koulakoff, S. Rudolph, M. Vitali, C. Giaume, F. Kirchhoff, M. Oheim, Systematic colocalization errors between acridine orange and EGFP in astrocyte vesicular organelles, Biophys. J. 93 (2007) 969–980, https://doi.org/10.1529/biophysj.106.102673.

[39] M.P. Thomé, E.C. Filippi-Chiela, E.S. Villodre, C.B. Migliavaca, G.R. Onzi, K. B. Felipe, G. Lenz, Ratiometric analysis of Acridine Orange staining in the study of acidic organelles and autophagy, J. Cell Sci. 129 (2016) 4622–4632, https://doi.org/10.1242/jcs.195057.

[40] D.M. Damas-Souza, R. Nunes, H.F. Carvalho, An improved acridine orange staining of DNA/RNA, Acta Histochem. 121 (2019) 450–454, https://doi.org/10.1016/j.acthis.2019.03.010.

[41] G.K. McMaster, G.G. Carmichael, Analysis of single- and double-stranded nucleic acids on polyacrylamide and agarose gels by using glyoxal and acridine orange, Proc. Natl. Acad. Sci. U. S. A. 74 (1977) 4835–4838, https://doi.org/10.1073/pnas.74.11.4835.

[42] J. Amagasa, Mechanisms of photodynamic inactivation of acridine orange-sensitized transfer RNA: participation of singlet oxygen and base damage leading to inactivation, J. Radiat. Res. 27 (1986) 339–351, https://doi.org/10.1269/jrr.27.339.

[43] V.A. Byvaltsev, L.A. Bardonova, N.R. Onaka, R.A. Polkin, S.V. Ochkal, V. V. Shepelev, M.A. Aliyev, A.A. Potapov, Acridine orange: a review of novel applications for surgical cancer imaging and therapy, Front. Oncol. 9 (2019) 925, https://doi.org/10.3389/fonc.2019.00925.

[44] A. Pierzyńska-Mach, P.A. Janowski, J.W. Dobrucki, Evaluation of acridine orange, LysoTracker Red, and quinacrine as fluorescent probes for long-term tracking of acidic vesicles, Cytometry 85 (2014) 729–737, https://doi.org/10.1002/cyto.a.22495.

[45] R. Chowdhury, S. Nandi, R. Halder, B. Jana, K. Bhattacharyya, Structural relaxation of acridine orange dimer in bulk water and inside a single live lung cell, J. Chem. Phys. 144 (2016), 065101, https://doi.org/10.1063/1.4941415.

[46] P. Slusarewicz, Z. Xu, K. Seefeld, A. Haas, W.T. Wickner, I2B is a small cytosolic protein that participates in vacuole fusion, Proc. Natl. Acad. Sci. U. S. A. 94 (1997) 5582–5587, https://doi.org/10.1073/pnas.94.11.5582.

[47] E. Harlow, D. Lane, Antibody purification on protein A or protein G columns, Cold Spring Harb. Protoc. (2006), https://doi.org/10.1101/pdb.prot4283 pdb.prot4283.

[48] S. Karunakaran, R.A. Fratti, The lipid composition and physical properties of the yeast vacuole affect the hemifusion-fusion transition, Traffic 14 (2013) 650–662, https://doi.org/10.1111/tra.12064.

[49] A. Haas, B. Conradt, W. Wickner, G-protein ligands inhibit in vitro reactions of vacuole inheritance, J. Cell Biol. 126 (1994) 87–97, https://doi.org/10.1083/jcb.126.1.87.

[50] O. Müller, H. Neumann, M.J. Bayer, A. Mayer, Role of the Vtc proteins in V-ATPase stability and membrane trafficking, J. Cell Sci. 116 (2003) 1107–1115, https://doi.org/10.1242/jcs.00328.

[51] G.E. Miner, K.D. Sullivan, C. Zhang, L.R. Hurst, M.L. Starr, D.A. Rivera-Kohr, B. C. Jones, A. Guo, R.A. Fratti, Copper blocks V-ATPase activity and SNARE complex formation to inhibit yeast vacuole fusion, Traffic 20 (2019) 841–850, https://doi.org/10.1111/tra.12683.

[52] N. Perzov, V. Padler-Karavani, H. Nelson, N. Nelson, Characterization of yeast V-ATPase mutants lacking Vph1p or Stv1p and the effect on endocytosis, J. Exp. Biol. 205 (2002) 1209–1219, https://doi.org/10.1242/jeb.205.9.1209.

[53] M.F. Manolson, B. Wu, D. Proteau, B.E. Taillon, B.T. Roberts, M.A. Hoyt, E. W. Jones, STV1 gene encodes functional homologue of 95-kDa yeast vacuolar H(+)-ATPase subunit Vph1p, J. Biol. Chem. 269 (1994) 14064–14074.

[54] S. Banerjee, K. Clapp, M. Tarsio, P.M. Kane, Interaction of the late endo-lysosomal lipid PI(3,5)P2 with the Vph1 isoform of yeast V-ATPase increases its activity and cellular stress tolerance, J. Biol. Chem. 294 (2019) 9161–9171, https://doi.org/10.1074/jbc.RA119.008552.

[55] S. Banerjee, P.M. Kane, Direct interaction of the Golgi V-ATPase a-subunit isoform with PI(4)P drives localization of Golgi V-ATPases in yeast, Mol. Biol. Cell 28 (2017) 2518–2530, https://doi.org/10.1091/mbc.E17-05-0316.

[56] A. Mayer, W. Wickner, A. Haas, Sec18p (NSF)-driven release of Sec17p (alpha-SNAP) can precede docking and fusion of yeast vacuoles, Cell 85 (1996) 83–94, https://doi.org/10.1016/s0092-8674(00)81084-3.

[57] J.-K. Ryu, D. Min, S.-H. Rah, S.J. Kim, Y. Park, H. Kim, C. Hyeon, H.M. Kim, R. Jahn, T.-Y. Yoon, Spring-loaded unraveling of a single SNARE complex by NSF in one round of ATP turnover, Science 347 (2015) 1485–1489, https://doi.org/10.1126/science.aaa5267.

[58] T. Söllner, M.K. Bennett, S.W. Whiteheart, R.H. Scheller, J.E. Rothman, A protein assembly-disassembly pathway in vitro that may correspond to sequential steps of synaptic vesicle docking, activation, and fusion, Cell 75 (1993) 409–418, https://doi.org/10.1016/0092-8674(93)90376-2.

[59] M. Zhao, S. Wu, Q. Zhou, S. Vivona, D.J. Cipriano, Y. Cheng, A.T. Brunger, Mechanistic insights into the recycling machine of the SNARE complex, Nature 518 (2015) 61–67, https://doi.org/10.1038/nature14148.

[60] A. Haas, W. Wickner, Homotypic vacuole fusion requires Sec17p (yeast alpha-SNAP) and Sec18p (yeast NSF), EMBO J. 15 (1996) 3296–3305.

[61] A.J. Merz, W.T. Wickner, Trans-SNARE interactions elicit Ca2+ efflux from the yeast vacuole lumen, J. Cell Biol. 164 (2004) 195–206, https://doi.org/10.1083/jcb.200310105.

[62] N. Thorngren, K.M. Collins, R.A. Fratti, W. Wickner, A.J. Merz, A soluble SNARE drives rapid docking, bypassing ATP and Sec17/18p for vacuole fusion, EMBO J. 23 (2004) 2765–2776, https://doi.org/10.1038/sj.emboj.7600286.

[63] R.A. Fratti, K.M. Collins, C.M. Hickey, W. Wickner, Stringent 3Q.1R composition of the SNARE 0-layer can be bypassed for fusion by compensatory SNARE mutation or by lipid bilayer modification, J. Biol. Chem. 282 (2007) 14861–14867, https://doi.org/10.1074/jbc.M700971200.

[64] K.M. Weixel, A. Blumental-Perry, S.C. Watkins, M. Aridor, O.A. Weisz, Distinct Golgi populations of phosphatidylinositol 4-phosphate regulated by phosphatidylinositol 4-kinases, J. Biol. Chem. 280 (2005) 10501–10508, https://doi.org/10.1074/jbc.M414304200.

[65] C. Stroupe, K.M. Collins, R.A. Fratti, W. Wickner, Purification of active HOPS complex reveals its affinities for phosphoinositides and the SNARE Vam7p, EMBO J. 25 (2006) 1579–1589, https://doi.org/10.1038/sj.emboj.7601051.
[66] R.A. Fratti, W. Wickner, Distinct targeting and fusion functions of the PX and SNARE domains of yeast vacuolar Vam7p, J. Biol. Chem. 282 (2007) 13133–13138, https://doi.org/10.1074/jbc.M700584200.
[67] M. Huss, G. Ingenhorst, S. König, M. Gassel, S. Dröse, A. Zeeck, K. Altendorf, H. Wieczorek, Concanamycin A, the specific inhibitor of V-ATPases, binds to the V (o) subunit c, J. Biol. Chem. 277 (2002) 40544–40548, https://doi.org/10.1074/jbc.M207345200.
[68] R. Wang, J. Wang, A. Hassan, C.-H. Lee, X.-S. Xie, X. Li, Molecular basis of V-ATPase inhibition by bafilomycin A1, Nat. Commun. 12 (2021) 1782, https://doi.org/10.1038/s41467-021-22111-5.
[69] J. Ciak, F.E. Hahn, Chloroquine: mode of action, Science 151 (1966) 347–349, https://doi.org/10.1126/science.151.3708.347.
[70] S. Tripathy, B. Dassarma, S. Roy, H. Chabalala, M.G. Matsabisa, A review on possible modes of action of chloroquine/hydroxychloroquine: repurposing against SAR-CoV-2 (COVID-19) pandemic, Int. J. Antimicrob. Agents 56 (2020), 106028, https://doi.org/10.1016/j.ijantimicag.2020.106028.
[71] K. Arai, A. Shimaya, N. Hiratani, S. Ohkuma, Purification and characterization of lysosomal H(+)-ATPase. An anion-sensitive v-type H(+)-ATPase from rat liver lysosomes, J. Biol. Chem. 268 (1993) 5649–5660.
[72] K.W. Cunningham, G.R. Fink, Calcineurin-dependent growth control in Saccharomyces cerevisiae mutants lacking PMC1, a homolog of plasma membrane Ca2+ ATPases, J. Cell Biol. 124 (1994) 351–363, https://doi.org/10.1083/jcb.124.3.351.
[73] K.W. Cunningham, G.R. Fink, Calcineurin inhibits VCX1-dependent H+/Ca2+ exchange and induces Ca2+ ATPases in Saccharomyces cerevisiae, Mol. Cell Biol. 16 (1996) 2226–2237, https://doi.org/10.1128/MCB.16.5.2226.
[74] V. Denis, M.S. Cyert, Internal Ca(2+) release in yeast is triggered by hypertonic shock and mediated by a TRP channel homologue, J. Cell Biol. 156 (2002) 29–34, https://doi.org/10.1083/jcb.200111004.
[75] G.E. Miner, K.D. Sullivan, A. Guo, B.C. Jones, L.R. Hurst, E.C. Ellis, M.L. Starr, R. A. Fratti, Phosphatidylinositol 3,5-bisphosphate regulates the transition between trans-SNARE complex formation and vacuole membrane fusion, Mol. Biol. Cell 30 (2019) 201–208, https://doi.org/10.1091/mbc.E18-08-0505.
[76] A. Chandel, K.K. Das, A.K. Bachhawat, Glutathione depletion activates the yeast vacuolar transient receptor potential channel, Yvc1p, by reversible glutathionylation of specific cysteines, Mol. Biol. Cell 27 (2016) 3913–3925, https://doi.org/10.1091/mbc.E16-05-0281.
[77] C. Poschenrieder, S. Busoms, J. Barceló, How plants handle trivalent (+3) elements, Int. J. Mol. Sci. 20 (2019) 3984, https://doi.org/10.3390/ijms20163984.
[78] X. Feng, Y. Huang, Y. Lu, J. Xiong, C.-O. Wong, P. Yang, J. Xia, D. Chen, G. Du, K. Venkatachalam, X. Xia, M.X. Zhu, Drosophila TRPML forms PI(3,5)P2-activated cation channels in both endolysosomes and plasma membrane, J. Biol. Chem. 289 (2014) 4262–4272, https://doi.org/10.1074/jbc.M113.506501.
[79] A. Bouron, K. Kiselyov, J. Oberwinkler, Permeation, regulation and control of expression of TRP channels by trace metal ions, Pflugers Arch - Eur J Physiol. 467 (2015) 1143–1164, https://doi.org/10.1007/s00424-014-1590-3.
[80] C.J. Herscher, A.F. Rega, Pre-steady-state kinetic study of the mechanism of inhibition of the plasma membrane Ca(2+)-ATPase by lanthanum, Biochemistry 35 (1996) 14917–14922, https://doi.org/10.1021/bi961879r.
[81] Y. Chen, J. Cao, J. Zhong, X. Chen, M. Cheng, J. Yang, Y. Gao, Plasma membrane Ca2+-ATPase regulates Ca2+ signaling and the proliferation of airway smooth muscle cells, Eur. J. Pharmacol. 740 (2014) 733–741, https://doi.org/10.1016/j.ejphar.2014.05.055.
[82] G.E. Miner, D.A. Rivera-Kohr, C. Zhang, K.D. Sullivan, A. Guo, R.A. Fratti, Reciprocal regulation of vacuolar calcium transport and V-ATPase activity, and the effects of Phosphatidylinositol 3,5-bisphosphate, bioRxiv (2020), https://doi.org/10.1101/2020.05.22.111153.
[83] K.A. Christensen, J.T. Myers, J.A. Swanson, pH-dependent regulation of lysosomal calcium in macrophages, J. Cell Sci. 115 (2002) 599–607, https://doi.org/10.1242/jcs.115.3.599.
[84] T. Fujimori, W.P. Jencks, Lanthanum inhibits steady-state turnover of the sarcoplasmic reticulum calcium ATPase by replacing magnesium as the catalytic ion, J. Biol. Chem. 265 (1990) 16262–16270, https://doi.org/10.1016/S0021-9258(17)46217-X.
[85] I. Jona, A. Martonosi, The effects of membrane potential and lanthanides on the conformation of the Ca2+-transport ATPase in sarcoplasmic reticulum, Biochem. J. 234 (1986) 363–371, https://doi.org/10.1042/bj2340363.
[86] A. Cohen, N. Perzov, H. Nelson, N. Nelson, A novel family of yeast chaperons involved in the distribution of V-ATPase and other membrane proteins, J. Biol. Chem. 274 (1999) 26885–26893, https://doi.org/10.1074/jbc.274.38.26885.
[87] M. Liu, M. Tarsio, C.M.H. Charsky, P.M. Kane, Structural and functional separation of the N- and C-terminal domains of the yeast V-ATPase subunit H, J. Biol. Chem. 280 (2005) 36978–36985, https://doi.org/10.1074/jbc.M505296200.
[88] A.J. Pope, R.A. Leigh, Dissipation of pH gradients in tonoplast vesicles and liposomes by mixtures of acridine orange and anions: implications for the use of acridine orange as a pH probe, Plant Physiol. 86 (1988) 1315–1322, https://doi.org/10.1104/pp.86.4.1315.
[89] J.E. DiCiccio, B.E. Steinberg, Lysosomal pH and analysis of the counter ion pathways that support acidification, J. Gen. Physiol. 137 (2011) 385–390, https://doi.org/10.1085/jgp.201110596.
[90] C.L. Brett, Y. Wei, M. Donowitz, R. Rao, Human Na(+)/H(+) exchanger isoform 6 is found in recycling endosomes of cells, not in mitochondria, Am. J. Physiol. Cell Physiol. 282 (2002) C1031–C1041, https://doi.org/10.1152/ajpcell.00420.2001.
[91] Q.-S. Qiu, R.A. Fratti, The Na+/H+ exchanger Nhx1p regulates the initiation of Saccharomyces cerevisiae vacuole fusion, J. Cell Sci. 123 (2010) 3266–3275, https://doi.org/10.1242/jcs.067637.
[92] E. Rabon, I. Kajdos, G. Sachs, Induction of a chloride conductance in gastric vesicles by limited trypsin or chymotrypsin digestion or ageing, Biochim. Biophys. Acta Biomembr. 556 (1979) 469–478, https://doi.org/10.1016/0005-2736(79)90134-2.